Progress In Electromagnetics Research M, Vol. 66, 87–98, 2018

Pattern Synthesis for the Cylindrical Polarimetric Phased Array Radar (CPPAR)

Mohammad-Hossein Golbon-Haghighi[1, *], Hadi Saeidi-Manesh[1], Guifu Zhang[1, 2], and Yan Zhang[1]

Abstract—A new optimization algorithm for the Cylindrical Polarimetric Phased Array Radar (CPPAR) antenna pattern synthesis is presented to achieve multi-mission requirements. To allow accurate weather measurements, the CPPAR antenna needs to have matched co-polarization (H and V) patterns, low sidelobe levels and high cross-polarization purity. To achieve these goals, first, a high-performance dual-polarized hybrid-fed microstrip patch antenna is designed, and its embedded radiation pattern is extracted. Then, a pattern synthesis using a new optimization method is presented to find the optimal weights for each radiating element and each polarization. The modified particle swarm optimization (MPSO) with new features is used to optimize the current distribution of the CPPAR. The adaptive beamforming algorithm also has the capability to mitigate interference by steering nulls of the radiation pattern in the desired direction without affecting the main beam. The performance improvement is demonstrated through the simulation results.

1. INTRODUCTION

The Multifunction Phased Array Radar (MPAR) is planned to integrate four radar networks in the United States. Replacing the (1) National Weather Surveillance Radar (WSR-88D or NEXRAD), (2) Terminal Doppler Weather Radar (TDWR), (3) Airport Surveillance Radar (ASR), and (4) Air Route Surveillance Radar (ARSR) with a single radar network would be cost-effective, beneficial, and will enable data sharing between radars [1–5]. Currently, the national weather surveillance radar has been upgraded with dual-polarization capability, and it is capable of transmitting and receiving both horizontally and vertically polarized waves simultaneously. The dual-polarization radar will improve weather measurements and classify hydrometeor types better than single polarized weather radars.

Compared to the traditional mechanically scanned antennas, which are currently used for weather measurements, phased array antennas offer faster data update and higher beam agility [6]. However, in a Planar Polarimetric Phased Array Antenna (PPPAR), the antenna radiation characteristics depend on the beam pointing angle, which results in a high level of cross-polarization in the off-principle plane scanning angles.

A cylindrical polarimetric phased array radar (CPPAR) has the advantages of azimuth scan-invariant pattern and polarization purity and has been proposed to overcome the deficiencies encountered with (PPPAR) [7]. However, the analysis and synthesis of the CPPAR antenna radiation pattern differ from that of PPPAR. The pattern synthesis for CPPAR is complicated because the element positions are not in one plane, and the array parameters are nonlinearly related to the element radiation pattern. Therefore, evolutionary optimization algorithms, including genetic algorithm (GA) [8, 9], particle swarm

Received 10 January 2018, Accepted 18 March 2018, Scheduled 26 March 2018

* Corresponding author: Mohammad-Hossein Golbon-Haghighi (golbon@ou.edu).

[1] School of Electrical & Computer Engineering, Advanced Radar Research Center (ARRC), The University of Oklahoma, USA.

[2] School of Meteorology, The University of Oklahoma, USA.

optimization (PSO) [10] and invasive weed optimization (IWO) [11–13], have been proposed to solve this optimization problem.

The first step in carrying out weather measurements is to generate a set of transmit beamforming weights for each embedded element pattern. However, finding these beamforming weights and pattern synthesis of nonplanar or cylindrical arrays is more complicated than for planar arrays. Several optimization algorithms for pattern synthesis have been recently proposed with smooth (parameterized) amplitude distributions, such as Bernstein polynomial [10, 13]. These algorithms use a predefined smooth amplitude distribution with fewer optimization variables and fewer degrees of freedom. Although these smooth amplitude distributions have a limited number of variables to be optimized (which reduces the optimization time and complexity), their optimization does not always converge for multi-objective optimizations. This is because the feasible sets of the optimization problem are bounded by reducing the number of optimization variables. Also, the optimization algorithms with smooth amplitude distributions cannot match the H and V co-polarization patterns, because the radiation patterns and embedded element patterns are not symmetric due to the mutual coupling effects. Furthermore, the beamforming optimization for null steering cannot be converged with the optimization methods based on the smooth amplitude distributions, because the radiation patterns and amplitude distributions are not symmetrical.

In this paper, an optimization algorithm for pattern synthesis is developed to efficiently optimize the beamforming weights of multi-objective optimization problem for the CPPAR. The beamforming weights are optimized to achieve the desired sidelobe levels, beam-width and matched horizontal and vertical co-polarization patterns. Also, an adaptive null steering feature is considered as another objective function for the optimization problem to reduce the effect of interference and ground clutter. Our novel optimization method is based on the particle swarm optimization (PSO) and is modified with an iterative particle replacing feature to improve computational efficiency and increase the convergence rate for our multi-objective optimization problem. For accurate weather measurements, it necessary to have low cross-polarization and high isolation antenna. A high-performance hybrid-fed dual-polarized microstrip patch antenna is also designed, and its embedded element pattern is used for cylindrical array pattern synthesis.

This paper is organized as follows: Section 2 presents the designed of single element. In Section 3, the formulation of the CPPAR antenna pattern is presented. In Section 4, the modified PSO algorithm is described. The optimization results along with the efficiency and specific features of this new algorithm are shown in Section 5. Conclusions are drawn in Section 6.

2. SINGLE ELEMENT DESIGN

In the presented hybrid feed design shown in Figure 1, horizontal polarization is excited by a balanced feed method which consists of a pair of 180° out of phase probes and a transmission line that distributes power from excitation point to the probes. The phase shift between two probes is provided by length difference of two arms of the horizontal polarization transmission line. Vertical polarization is excited

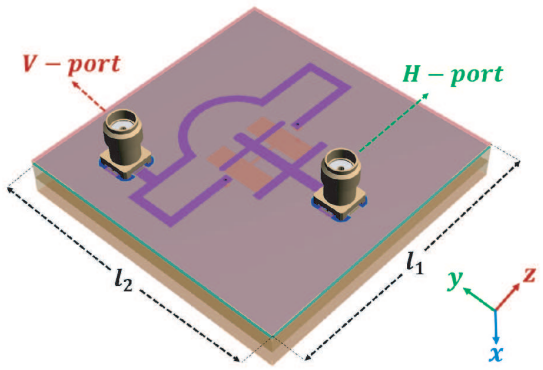

Figure 1. The geometry of the designed hybrid-fed microstrip patch antenna $l_1 = l_2 = 55\,\text{mm}$.

through an H-shaped slot which is placed in the center of the ground plane. The H-shaped slot is fed by a transmission line laid below the ground plane. Also, since the bandwidth of the microstrip patch antenna is limited, a parasitic square patch with a smaller dimension is placed on top of the excited radiating square patch. In this design, the transmission lines are laid on a top layer of the first substrate which is a 1.574 mm thick Rogers 5880. The ground plane is etched and on the bottom layer of the first substrate. The excited radiation patch and parasitic patch are laid on the bottom side of the second and third substrates, which are 3.175 mm thick Rogers 5880.

The simulated S-parameter of the designed single element is shown in Figure 2. As shown in Figure 2 the reflection coefficient of horizontal and vertical polarizations are below -13 dB, and isolation between horizontal and vertical ports is more than 52 dB. For array radiation pattern synthesis, the embedded

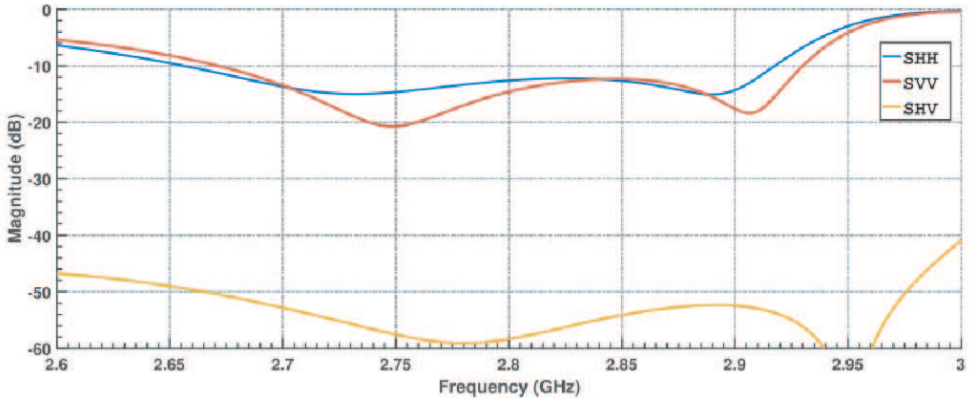

Figure 2. Simulated reflection coefficient and isolation of horizontal and vertical ports.

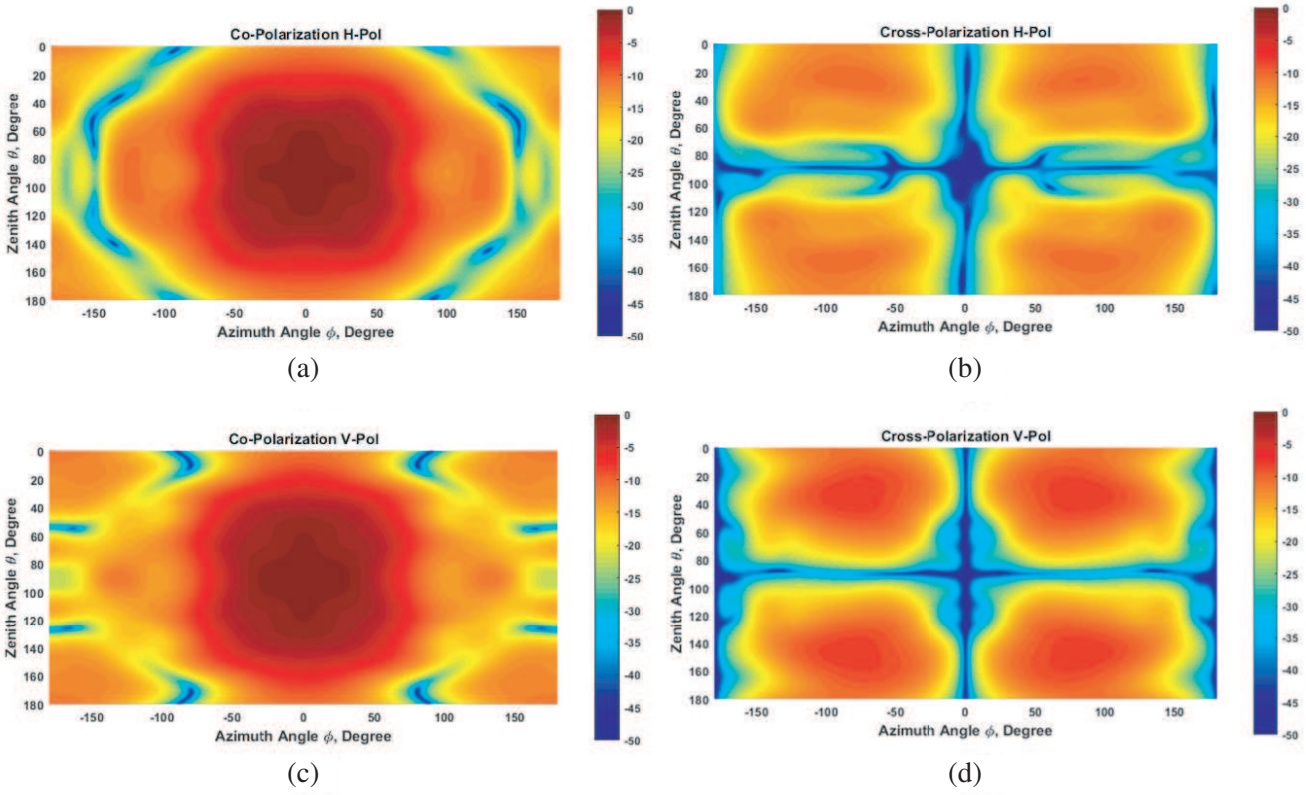

Figure 3. Embedded co and cross-polarization radiation pattern of the designed single element.

element pattern of the designed element is used. The advantage of using embedded element pattern is that the coupling between elements will be included in the element radiation pattern and the array radiation pattern will be more accurate and closer to full-wave simulations than using an isolated element pattern for calculating the array radiation pattern. Since the embedded element radiation pattern of the large cylindrical array antenna is similar to the embedded element radiation pattern of the planar array antenna, the embedded element pattern is extracted from the simulation of 5×5-element planar array antenna while the center element was excited and all other elements were terminated. The embedded element pattern of the designed element is shown in Figure 3.

3. PATTERNS OF CYLINDRICAL ARRAYS

The analysis and synthesis of nonplanar arrays are more complicated than the analysis and synthesis of planar arrays because the element positions are not in one plane, and the effective element spacings are not always equal. In cylindrical array antennas, the array factor and element patterns are not separable, and the array factor is not simple as it is for planar arrays. A cylindrical array has the advantage of symmetry in azimuth, making it a natural fit for applications with a full 360° coverage. The CPPAR beam and polarization characteristics do not change when a commutation scan is performed. A CPPAR schematic is shown in Figure 4.

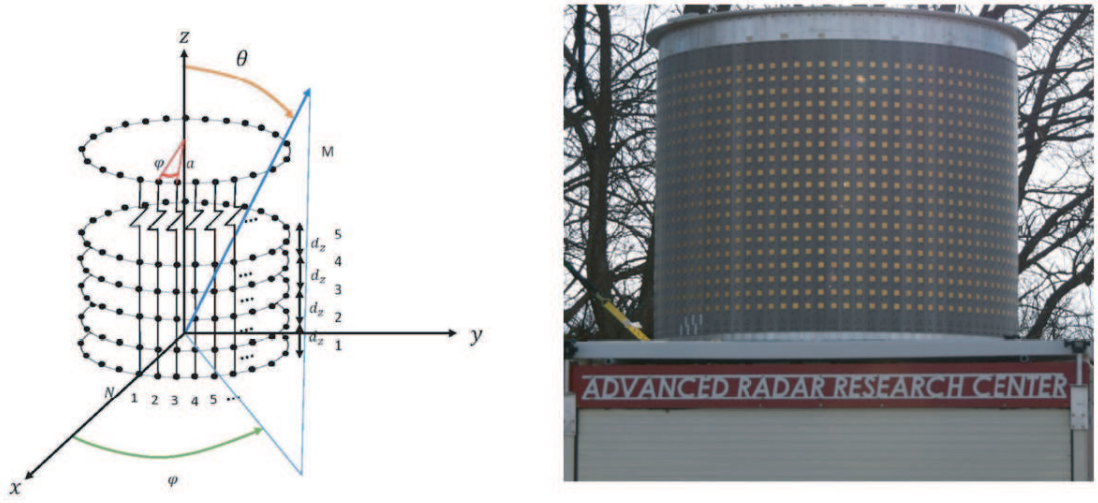

(a) (b)

Figure 4. Cylindrical polarimetric phased array radar; (a) schematic; (b) CPPAR.

The radiation pattern for CPPAR with radius of "r" and N elements located on a circumference of a cylinder at $(\varphi_n = n\Delta\varphi, Z_m)$ can be simply calculated as [14, 15].

$$E(\theta,\varphi) = \sum_{m=1}^{M}\sum_{n=1}^{N} w(n,m)F_{n,m}(\theta,\varphi)e^{jk(r\sin\theta\cos(\varphi-n\Delta\varphi))+z_m\cos(\theta)} \tag{1}$$

where N and M are the numbers of elements in H and E-planes; $w(n,m)$ is the amplitude excitation of the nmth element; $F_{n,m}(\theta,\varphi)$ are the active element patterns; φ_n, z_m are the location of nmth element on the cylindrical coordinate system. Also, the element patterns of CPPAR are dependent on the element location and due to symmetry, it can be written as:

$$F_{n,m}(\theta,\varphi) = f(\theta,\varphi - n\Delta\varphi) \tag{2}$$

The amplitude excitation $w(n,m)$ contains the amplitude and phase required for array radiation pattern synthesis. For in-phase collimated beam at the angle (θ_0,φ_0), we have:

$$w(n,m)F_{n,m} = |w(n,m)F_{n,m}(\theta,\varphi)|e^{-jkr\sin\theta_0\cos(\varphi_0-n\Delta\varphi)} \tag{3}$$

It should be noted that the CPPAR array can be focused on the elevation angle that is not necessarily broadsided or in the plane of the array ($\theta_0 = \pi/2$). Therefore, the array pattern for the cylindrical array in (θ_0, φ_0) direction would be:

$$E(\theta,\varphi) = \sum_{m=1}^{M}\sum_{n=1}^{N} w(n,m) F_{n,m}(\theta,\varphi) e^{jk((r\sin\theta\cos(\varphi - n\Delta\varphi)) + z_m\cos(\theta)) - (r\sin\theta_0\cos(\varphi_0 - n\Delta\varphi)) + z_m\cos(\theta_0))} \quad (4)$$

4. MODIFIED PARTICLE SWARM OPTIMIZATION

In this section, the particle swarm optimization (PSO) is modified and applied to the CPPAR antenna to obtain the radiation pattern with the desired sidelobe levels (SLL). Particle swarm optimization simulates the behaviors of bird flocking [16–18]. In this algorithm, a group of birds is randomly searching for food in the specific area. There is only one piece of food in the area being searched [10, 19]. Although all the birds do not know where the food is, they know their distance to the food, in each step. In our case, one set of beamforming weight w in Eq. (4) represents a particle for the optimization problem. The distance of the array radiation pattern to desired radiation pattern (i.e., mask) for each w is defined as the distance of the particle to the food or the fitness value. Thus, the best strategy to find the food or optimal value is to follow the bird which is nearest to the food. PSO is learning from the scenario and updating particles to solve the optimization problem. In this algorithm, every single solution is considered as a particle in the solution space. All the particles have fitness values which are evaluated by the optimal value and have velocities which direct the flying of the particles to the food. The particles follow the current optimum particle (or local best) and fly through the problem space to find the global optimal value (or global best). Consider $2N$ variables as the phase and amplitude of N element patterns for the optimization. Each particle is assigned a random position in the $2N$-dimensional problem space and represents one set of beamforming weights. Therefore, each particle's position is corresponding to a candidate solution of the optimization problem, and these particle positions are scored to calculate a cost based on how well each particle solves the problem. By using a simple update rule, these particles then fly to new positions in the problem space, which are then mapped to the problem space and scored in new positions.

In each step, each particle knows the best position that it has ever found, named as the local best. Each particle also knows the best position found by any other particles, named as the global best. By proceeding optimization, particles are pulled toward these known solutions with linear spring-like attraction forces [10]. In general, PSO starts by initializing a group of particles (here 40), with random positions. The random values are between 0 and 1. In some cases, the initial points can be defined as deterministic distributions such as Taylor or Chebyshev distributions. The object of the optimization problem is to obtain sidelobe levels less than a tapered mask and holding the 3-dB beamwidth to be around 2° and matched copolar patterns. Then, all these particles are scored to find the global best particle.

Finally, by using the following stochastic velocity update rule, the particles are flown through the problem hyperspace for a specified number of iterations.

$$\nu_{k+1} = w\nu_k + \phi_1 \text{rand}\left(p_k^{\text{local best}} - p_k\right) + \phi_2 \text{rand}\left(p_k^{\text{global best}} - p_k\right) \quad (5)$$

where p_k is the position of the kth particle, $p_k^{\text{local best}}$ the best position ever found by p_k, $p_k^{\text{global best}}$ the best position of any particle, v_k the velocity of the kth particle, w the inertia or momentum, and ϕ_1 and ϕ_2 are the self-knowledge and group knowledge weights and also known as correction factors. Inertia is proportional to the old velocity and is the tendency of the particle to continue in the same direction it has been traveling. It is possible to select this multiplier as a random value or decreasing function to encourage local searching at the end of the optimization process or randomly vary during the optimization [10]. In our case, w is assumed to be a constant value: $w = 0.2$.

In each iteration, the second term of the velocity (i.e., $\phi_1 \text{rand}(p_k^{\text{local best}} - p_k)$) is updating like a linear attraction toward the best position ever found by a particle (local best) and scaled by a constant value and a random number. The third term of the velocity (i.e., $\phi_2 \text{rand}(p_k^{\text{global best}} - p_k)$) is updating the equation as a linear attraction toward the best position found by any particle (global best) and

scaled by a constant and a random number between zero and one. For this study, the correction factors are assumed to be: $\phi_1 = \phi_2 = 2$. It should be noted that a high value of ϕ_1, ϕ_2 can cause the particles to converge quickly on a solution, but cannot cover enough of the solution space. If the correction factors are too low, the swarm will lose consistency, and it will be difficult to converge on a solution space. Finally, the new position of the particle is calculated as:

$$p_{k+1} = p_k + \nu_k \tag{6}$$

It should be noticed that the beamforming weights should be optimized to achieve the desired sidelobe levels, 2° beamwidth, matched horizontal and vertical co-polarization patterns and null steering. Therefore, for this multi-objective optimization, some of the particles have never converged to the optimal value, as discussed in the next section. Therefore, the convergence rate can be improved by replacing these particles with new particles. Consequently, PSO is modified with a new feature to eliminate the particles with lower fitness values and replaced them with new particles, every m iterations. The new particles are spread over the solution space, as shown in Figure 5. This feature can improve the optimization performance, especially for multi-objective optimization problem.

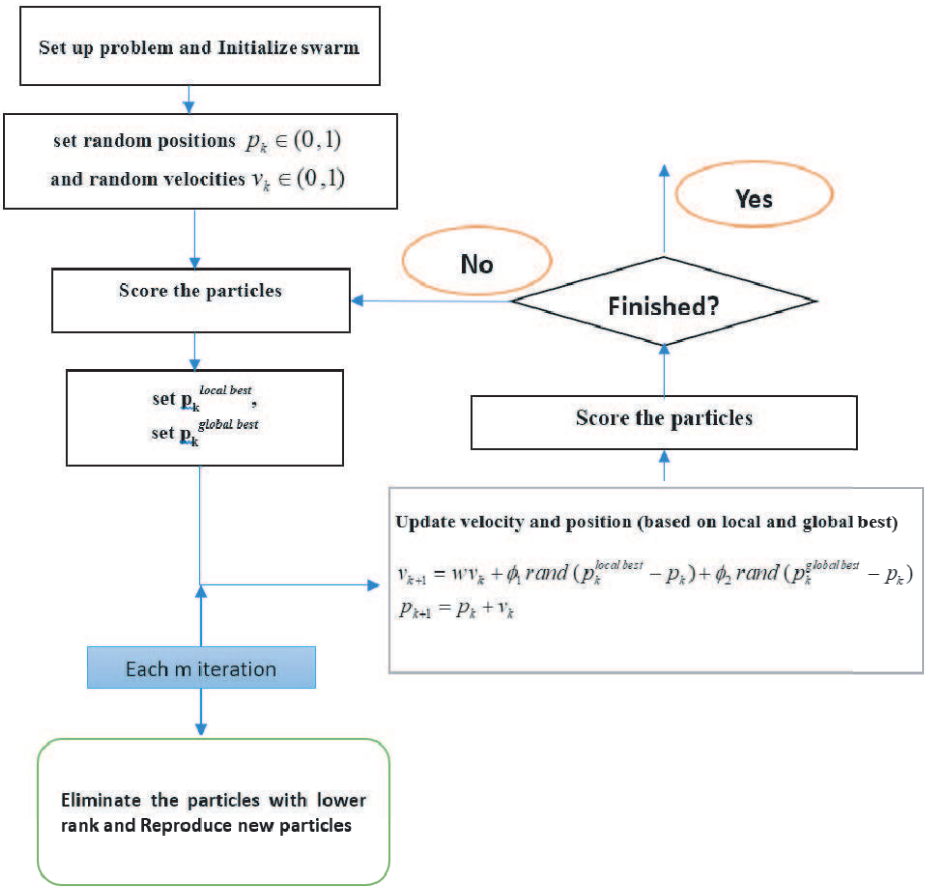

Figure 5. Flowchart of the optimization algorithm.

5. OPTIMIZATION RESULTS

For the optimization problem, multi-objective functions have been considered [20–22]. The modified PSO algorithm is designed to match the main beams and keep the beamwidth around 2° while minimizing the sidelobe levels (SLL). It is important to match the main beams because the mismatch could result in inaccurate weather sensing. Coupling effect in the element pattern is the reason for obtaining different patterns for horizontal- and vertical-polarized beams. Therefore, in each m iterations,

the particles with the beamwidth, far from 2°, will be replaced by new particles. New particles are replaced over the solution space, near the global best. Therefore, new particles are distributed in random positions with mean equal to the global best and varying standard deviations.

Also, the optimization algorithm has been designed to match the main beam of H and V polarizations and also to keep all pattern peaks at the same levels compared to the mask, in order to smooth out the amplitude distribution.

$$\begin{aligned} &\underset{w}{\text{Minimize}}: \quad \text{SLL}_{H,V} \\ &\text{Subject to } BW_{H,V} = 2 \\ &MB_{H,V} \approx 0 \end{aligned} \tag{7}$$

where w stands for the beamforming weights, $\text{SLL}_{H,V}$ the maximum SLLs for H and V polarizations compared to the mask, $BW_{H,V}$ the 3-dB beamwidths of radiation patterns for H and V polarizations, and $MB_{H,V}$ the difference between main beam levels for H and V polarizations that should be matched during the optimization, as shown in Figure 6. For simplicity, Eq. (7) can be rewritten based on the

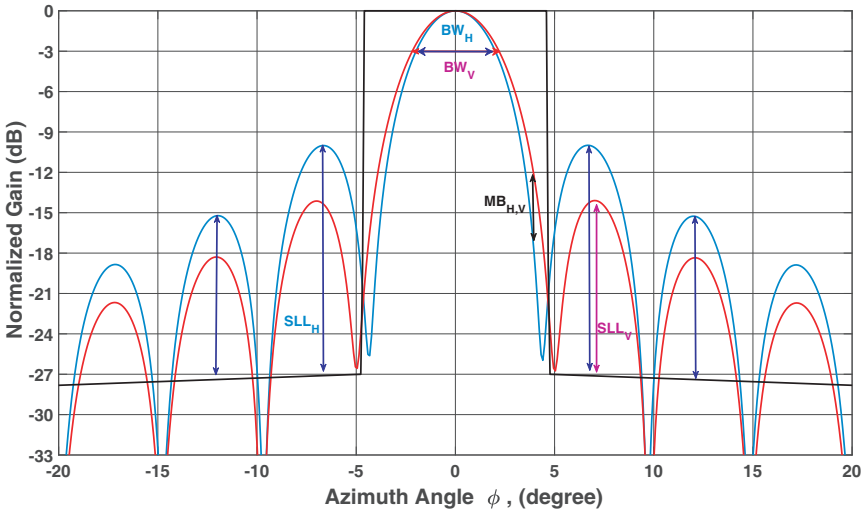

Figure 6. Multi-objective optimization.

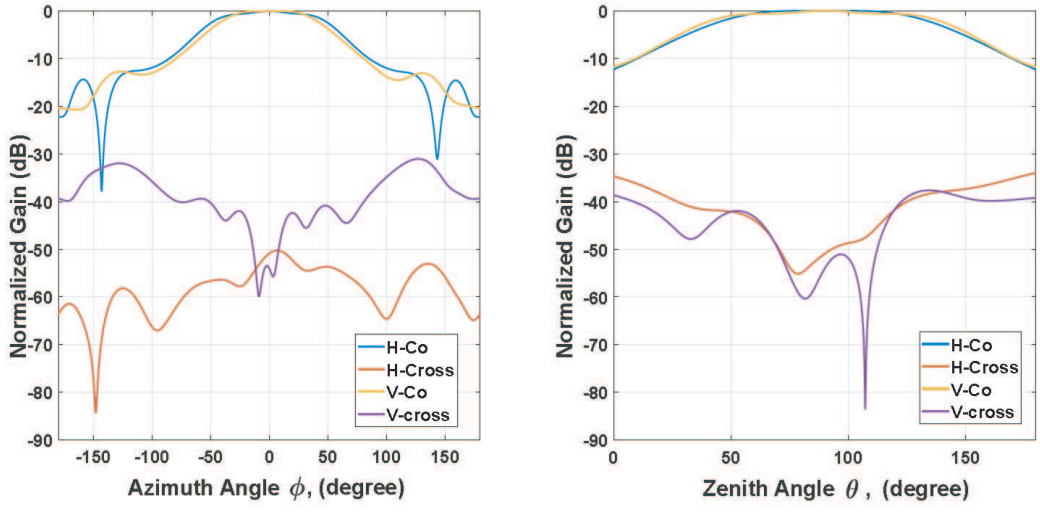

Figure 7. Embedded element pattern in (a) horizontal plane and (b) vertical plane.

Lagrangian method:

$$\underset{w}{\text{Minimize}}: \quad \text{SLL}_{H,V} + \lambda_1 \left(|BW_{H,V} - 2|\right) + \lambda_2(|MB_{H,V}|) \tag{8}$$

where λ_1 and λ_2 are the normalized coefficient for the optimization problem.

Figure 7, shows the embedded element pattern for H and V polarizations. The optimized radiation patterns at frequency 2.8 GHz are shown in Figure 8, in the horizontal plane for H and V polarizations. The beamforming weights are optimized to achieve 2° beamwidth with matched H and V polarizations with respect to the pre-defined mask. A 90° sector of cylinder surface needs to populate with 70 columns around the cylinder and 53 elements in each vertical column to achieve all optimization goals, based on the optimization results. Also, the element spacing in the horizontal plane is chosen by the optimization program to be 0.58λ. Having such a spacing between elements, a CPPAR design is achieved with a height of 3.23 m and a radius of $R = 2.72$ m.

The mask is defined to increase from −27 dB to −34 dB at 135°. Figure 9 shows the optimized radiation pattern for H polarization in H-plane compared to Taylor distribution (4, −30) with the same beamwidth. It can be seen from this figure that our modified PSO algorithm has around 4 dB gain improvement in SLL compared to Taylor distribution, for the same beamwidth and matched co-

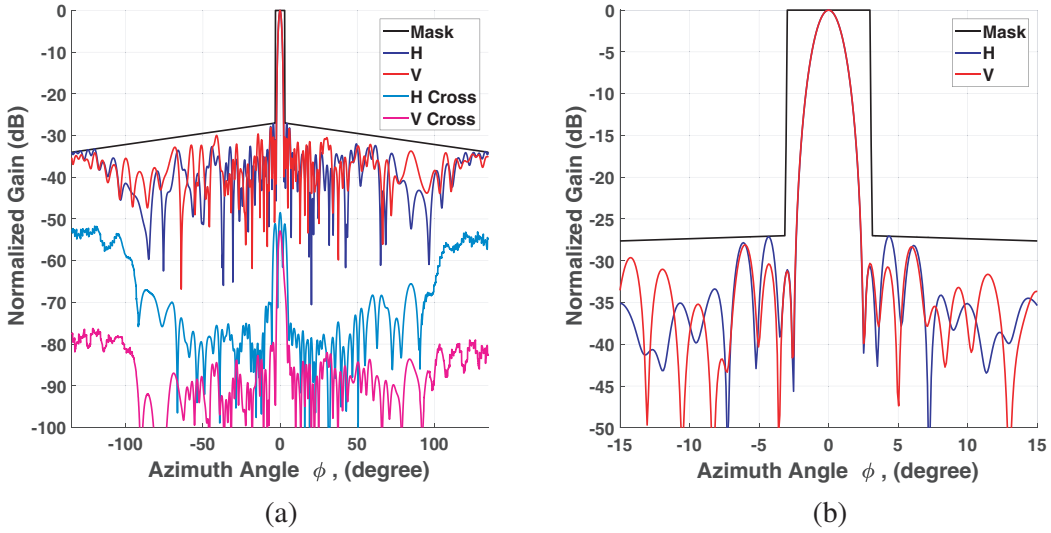

Figure 8. Optimized radiation pattern in horizontal plane.

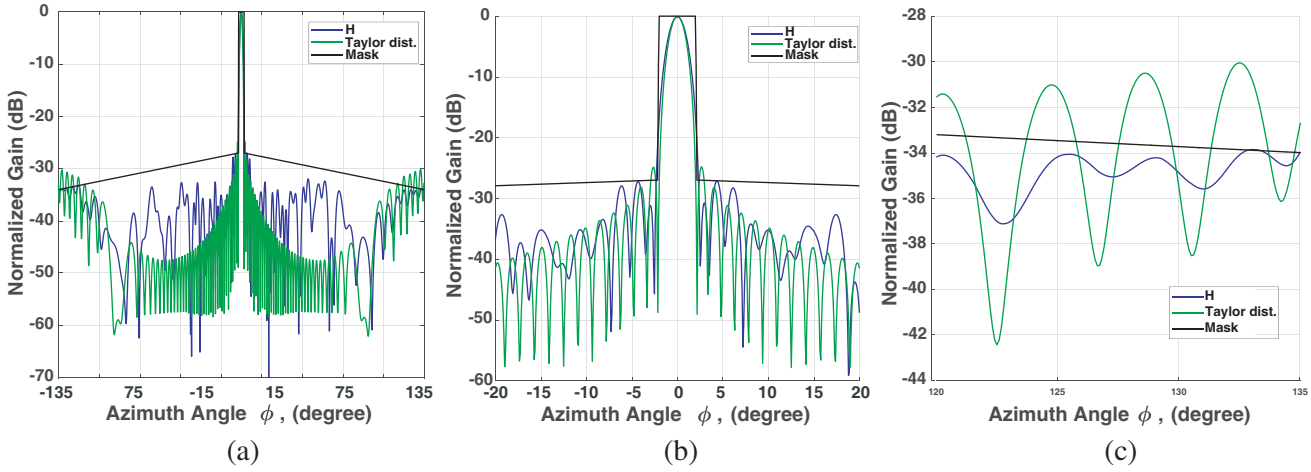

Figure 9. Optimized radiation pattern in horizontal plane compare to Taylor distribution.

polar patterns. It should be noted that the beamwidth could be reduced at the cost of increasing the sidelobe levels. However, the goal of the optimization is to achieve relatively low SLL and 2-degree beamwidth while having the matched main beams for H and V polarizations.

Achieving both lower SLLs and reducing the beamwidth can be obtained by increasing the antennas aperture, which can cause grating lobes to appear. Therefore, we can decrease the beamwidth by either increasing the spacing of elements or increasing the number of elements. Therefore, the optimization problem is designed to compromise between the spacing, SLL, and beamwidth, while co-polar patterns are matched. The current distribution of the radiation pattern in the horizontal plane may not be symmetrical because the embedded element patterns are not symmetrical since the patch on each column is not designed to be in the middle of the antenna column. Furthermore, the current distribution is achieved using an evolutionary optimization algorithm which does not provide a unique solution to the optimization problem [11].

Also, the PSO algorithm needs to optimize all 70 elements separately. It is clear that getting all of the sidelobe levels below a certain level, holding the beamwidth around 2° and matching the main beams for H and V polarizations by using the optimization algorithm results in an asymmetrical current

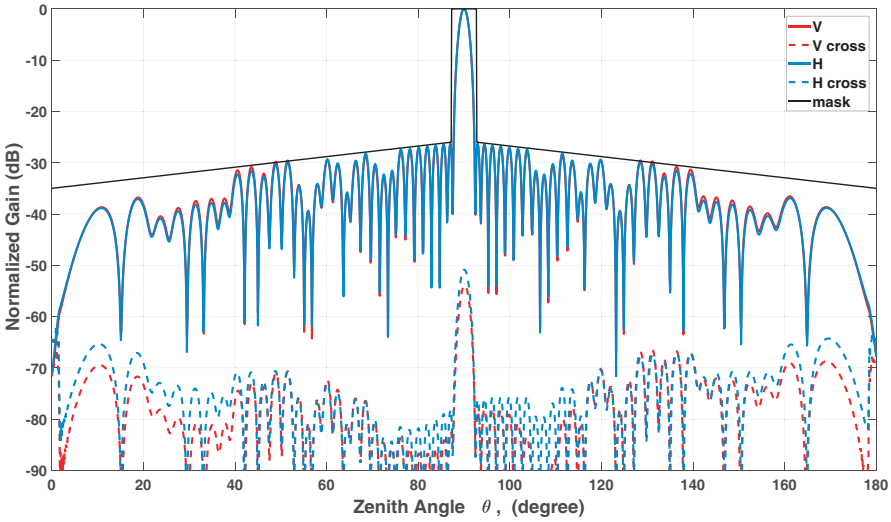

Figure 10. Optimized radiation pattern in vertical plane for H and V polarizations.

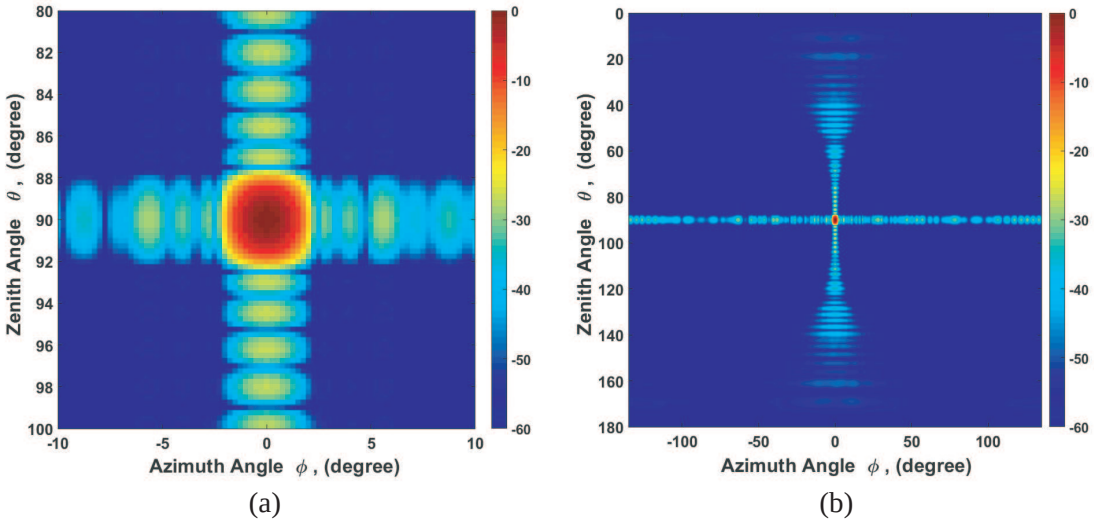

Figure 11. Optimized 2D co-polar radiation pattern for H polarization.

distribution. This will not affect the practical implantation of the array since any current value can be applied to the antenna column using the amplifiers [11]. Also, we can use another constraint to smooth out the amplitude distribution, in the case it has practical limitations.

It should be noted that there are several smooth current distributions, like the Taylor distribution or Bernstein polynomial, with a fewer optimization variables and less degrees of freedom. However, these distributions have a limited number of variables to be optimized, so it can easily limit the optimization performance, especially for multi-objective optimizations.

Figure 10 shows the co- and cross-polar radiation patterns in the vertical plane for H and V polarizations with 53 elements. The beamwidth for both H-pol and V-pol is designed to be 2°. Figure 11 shows the optimized 2D copolar radiation pattern for designed CPPAR. To achieve a cost-efficient design for the CPPAR, the number of elements should be minimized. To minimize the number of elements for array antennas, element spacing should be increased, which can cause the appearance of grating lobes. Therefore, we need to compromise between the number of elements and appearance of grating lobes, based on the specific case. It is clear that the 3-dB beamwidth will increase by decreasing the number

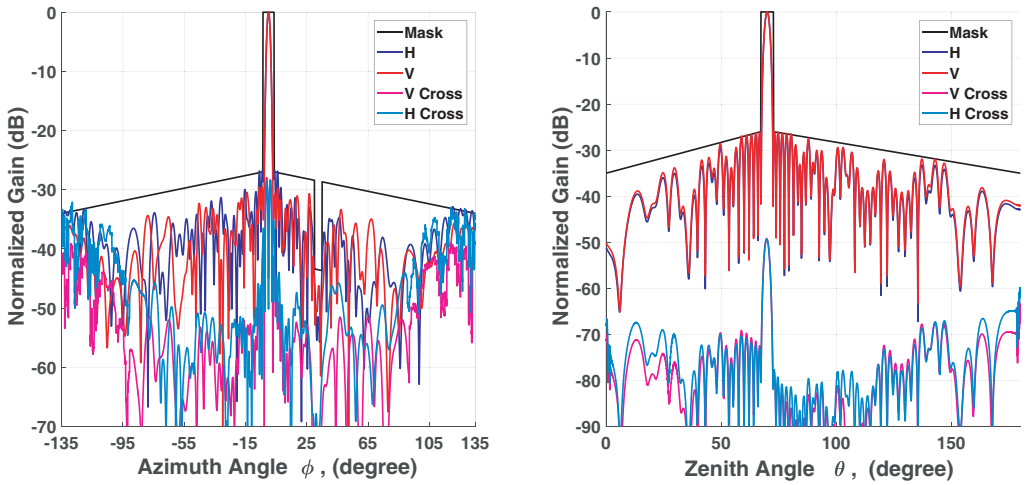

Figure 12. Optimized radiation pattern in (a) horizontal plane and (b) vertical plane for H and V polarizations with 20-degree elevation.

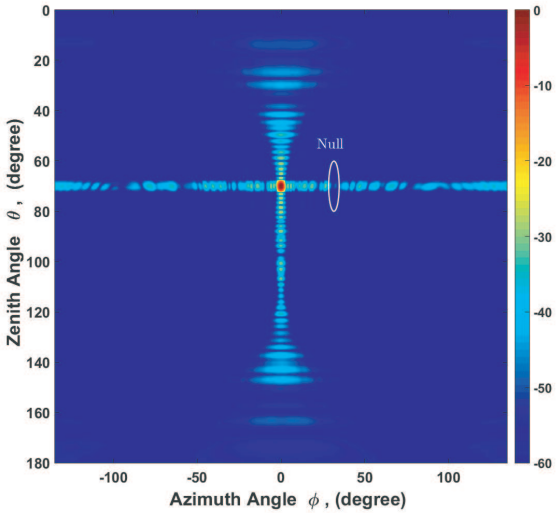

Figure 13. Optimized 2D co-polar radiation pattern for 20-degree elevation.

of elements in the vertical or horizontal planes.

To study the performance of the proposed modified PSO algorithm for other elevations, a 20° elevation has been considered. Here, the modified PSO is designed to achieve the desired sidelobe level, beamwidth and matched co-polarization patterns, while the main beam is pointed to $\theta = 70°$. Also, a null is steered with 15 dB lower than the mask and between 30°–35°, as shown in Figure 12. The radiation pattern in the horizontal and vertical planes for H and V polarizations are optimized for the case where the main beam is pointed to $\theta = 70°$. It is clear that by increasing the scan angle in elevation, the beamwidth was slightly increased, for the same number of elements and side lobe levels. The 2D copolar radiation pattern for 20° elevation is shown in Figure 13. The optimization algorithm can update the beamforming weights to have null steering for different directions and widths, if we have interference from more than one directions. To mitigate the back-to-back interference when multiple simultaneous beams are formed and share the same frequency, a null can be designed at 180°.

6. CONCLUSION

A modified PSO algorithm was applied to optimally design the cylindrical polarimetric phased array radar (CPPAR) antenna patterns for weather measurements. After minimizing the number of elements of the CPPAR, the complex beamforming weights are optimized to achieve the desired radiation pattern based on the multi objective function. Simulation results show the performance of the modified PSO algorithm in achieving desired sidelobe levels and beamwidth and matched co-polarization patterns, for both broadside and off broadside directions. Also, an adaptive null steering feature is considered to reduce the effect of interference and ground clutter.

ACKNOWLEDGMENT

This work was supported by the National Oceanic and Atmospheric Administration under Grants NA11OAR4320072 and NA16OAR4320115.

REFERENCES

1. Weber, M., J. Cho, J. Flavin, J. Herd, and M. Vai, "Multi-function phased array radar for US civil-sector surveillance needs," *The 32nd Conf. on Radar Meteorology*, Albuquerque, NM, Oct. 24–29, 2005.
2. Zrnic, D., J. Kimpel, D. Forsyth, A. Shapiro, G. Crain, R. Ferek, J. Heimmer, W. Benner, T. McNellis, and R. Vogt, "Agile-beam phased array radar for weather observations," *Bulletin of the American Meteorological Society*, Vol. 88, No. 11, 1753–1766, 2007.
3. Zhang, G., *Weather Radar Polarimetry*, CRC Press, 2016.
4. Saeidi-Manesh, H. and G. Zhang, "Characterization and optimization of cylindrical polarimetric array antenna patterns for multi-mission applications," *Progress In Electromagnetics Research*, Vol. 158, 49–61, 2017.
5. Golbon-Haghighi, M.-H., Y. Li, G. Zhang, and R. Doviak, "Detection of ground clutter from weather radar using a dual-polarization and dual-scan method," *Atmosphere*, Vol. 7, No. 6, 83, Jun. 2016.
6. Saeidi-Manesh, H., S. Karimkashi, G. Zhang, and R. J. Doviak, "High-isolation low cross-polarization phased-array antenna for mpar application," *Radio Science*, Vol. 158, 49–61, 2017.
7. Saeidi-Manesh, H. and G. Zhang, "Cross-polarisation suppression in cylindrical array antenna," *Electronics Letters*, Vol. 53, No. 9, 577–578, 2017.
8. Yang, J. O., Q. R. Yuan, F. Yang, H. J. Zhou, Z. P. Nie, and Z. Q. Zhao, "Synthesis of conformal phased array with improved NSGA-II algorithm," *IEEE Transactions on Antennas and Propagation*, Vol. 57, No. 12, 4006–4009, Dec. 2009.
9. Holland, J. H., "Genetic algorithms," *Scientific American*, Vol. 267, No. 1, 66–73, 1992.

10. Boeringer, D. W. and D. H. Werner, "Efficiency-constrained particle swarm optimization of a modified bernstein polynomial for conformal array excitation amplitude synthesis," *IEEE Transactions on Antennas and Propagation*, Vol. 53, No. 8, 2662–2673, 2005.
11. Karimkashi, S. and G. Zhang, "Optimizing radiation patterns of a cylindrical polarimetric phased-array radar for multimissions," *IEEE Transactions on Geoscience and Remote Sensing*, Vol. 53, No. 5, 2810–2818, May 2015.
12. Saeidi-Manesh, H. and G. Zhang, "High-isolation, low cross-polarization, dual-polarization, hybrid feed microstrip patch array antenna for MPAR application," *IEEE Transactions on Antennas and Propagation*, Vol. 66, No. 05, 2018, doi: 10.1109/TAP.2018.2811780.
13. Karimkashi, S. and G. Zhang, "An optimal design of a cylindrical polarimetric phased array radar for weather sensing," *Radio Science*, Vol. 47, No. 2, 2012.
14. Mailloux, R. J., *Phased Array Antenna Handbook (Artech House Antennas and Propagation Library)*, Artech House, 2005.
15. Lei, L., G. Zhang, and R. J. Doviak, "Theoretical analysis of polarization characteristics for planar and cylindrical phased array radars," *AMS General Meeting in New Orleans*, 2012.
16. Eberhart, R. and J. Kennedy, "A new optimizer using particle swarm theory," *Proceedings of the Sixth International Symposium on Micro Machine and Human Science, 1995, MHS'95*, 39–43, IEEE, 1995.
17. Kennedy, J., "Particle swarm optimization," *Encyclopedia of Machine Learning*, 760–766, Springer, 2011.
18. Eberhart, R. C., Y. Shi, and J. Kennedy, *Swarm Intelligence*, Elsevier, 2001.
19. Khodier, M. M. and M. Al-Aqeel, "Linear and circular array optimization: A study using particle swarm intelligence," *Progress In Electromagnetics Research B*, Vol. 15, 347–373, 2009.
20. Golbon-Haghighi, M. H., B. Mahboobi, and M. Ardebilipour, "Linear pre-coding in MIMO-CDMA relay networks," *Wireless Personal Communications*, Vol. 79, No. 2, 1321–1341, Springer, Jul. 2014.
21. Golbon-Haghighi, M. H., "Beamforming in wireless networks," *InTech Open*, Book Chapter, 163–192, ISBN 978-953-51-2833-5, Dec. 2016.
22. Golbon-Haghighi, M. H., B. Mahboobi, and M. Ardebilipour, "Multiple antenna relay beamforming for wireless peer to peer communications," *Journal of Information Systems and Telecommunication (JIST)*, 209–2015, 2013.